LIMNOLOGY and OCEANOGRAPHY

ASLO

Limnol. Oceanogr. 63, 2018, S367–S380

doi: 10.1002/lno.10745

The physiological response of seven strains of picophytoplankton to light, and its representation in a dynamic photosynthesis model

Beate Stawiarski [1,2]* **Erik T. Buitenhuis,** [1] **Mehera Fallens** [1]

[1]School of Environmental Sciences, University of East Anglia, Norwich, UK

[2]Leibniz Institute for Baltic Sea Research, Warnemünde, Rostock, Germany

Abstract

Picophytoplankton dominate the phytoplankton community in wide ocean areas and are considered efficient in the acquisition of light compared to other phytoplankton groups. To quantify their photophysiological parameters we use three strains of picoprokaryotes and four strains of picoeukaryotes. We measure the acclimated response of the exponential growth rates and chlorophyll *a* (Chl *a*) to carbon ratios, as well as the instantaneous response of photosynthesis rates at 5–7 light intensities. We then use a dynamic photosynthesis model (Geider et al. 1997) and extend it with a photoinhibition term. We derive five photophysiological parameters: the maximum rate of photosynthesis (P_m^C), the affinity to light (α^{chl}), the photoinhibition term (β^{chl}), the respiration rate (resp), and the maximum Chl *a* to carbon ratio (θ_{max}). We show that P_m^C is significantly lower for picoprokaryotes than for picoeukaryotes and increases significantly with increasing cell size. In turn, α^{chl} decreases significantly with increasing maximum growth rate (μ_{max}). The latter finding is contrary to a previously reported relationship for phytoplankton, but agrees with theoretical assumptions based on size. The higher efficiency in light acquisition gives picoprokaryotes an advantage in light limited environments at the expense of their maximum growth rate. In addition, our results indicate that the accumulation of long-term damage through photoinhibition during acclimation is not well represented by the dynamic photosynthesis model. Hence, we would recommend to distinguish between the effects of irreversible damage (on a time scale of days) on growth rates and of reversible damage (on a time scale of minutes) on photosynthesis rates.

Picophytoplankton include cells with a diameter ≤ 3 μm (e.g., Vaulot et al. 2008) and consist of two distinct groups: picoprokaryotes represented by *Prochlorococcus* and *Synechococcus*, and picoeukaryotes with representatives from diverse phytoplankton classes. Both groups contribute substantially to phytoplankton biomass (Buitenhuis et al. 2013), primary production (Grossman et al. 2010), and to the recycling of organic matter within the microbial loop in the surface ocean (Azam et al. 1983; Fenchel 2008). They are found in all marine environments and dominate the oligotrophic ocean areas. Both picoprokaryotes are more abundant than picoeukaryotes (Veldhuis et al. 2005), but constitute a smaller biomass (Buitenhuis et al. 2012). In contrast to bloom forming phytoplankton, such as diatoms, picophytoplankton generally have a more constant biomass, which was suggested to be due to compensation of mortality rates with reproduction (Massana and Logares 2013). Altogether, picophytoplankton may extend their dominance in the phytoplankton community with global warming (Morán et al. 2010), in part as a consequence of their efficient light acquisition (Raven 1998) in light limited environments such as deep stratified ocean waters.

Light has a strong effect on the physiological response of individual phytoplankton groups and hence on the composition of the phytoplankton community (Boyd et al. 2010). The particular effects of light can be quantified by measuring the acclimated response of exponential growth rates or the instantaneous response of photosynthesis rates of individual phytoplankton groups or strains to different light intensities (Platt et al. 1980). Light also affects the cellular composition of the phytoplankton cells, due to acclimation to the prevailing conditions. It changes the major nutrient stoichiometry of carbon, nitrogen, and phosphorus as well as chlorophyll *a* (Chl *a*) (Geider 1987; Sterner and Elser 2002). Thus, the acclimation to high light intensities leads to a decline in Chl *a*, but to an increase of energy storage components (Geider 1987), which in turn affects the growth and photosynthesis rates.

*Correspondence: beate.stawiarski@io-warnemuende.de

Additional Supporting Information may be found in the online version of this article.

Picophytoplankton have distinct photophysiological characteristics. The picoprokaryote *Prochlorococcus* sp. reaches the smallest possible size, while containing all essential photosynthetic and metabolic apparatus (Raven 1998). It includes low-light and high-light adapted ecotypes which are characterized by differences in pigment composition (Partensky et al. 1999). Picoeukaryotes include a variety of taxa with more complex cells, different pigment compositions and individual photophysiological characteristics. Previous studies described the photophysiology of picophytoplankton (e.g., Glover et al. 1987; Partensky et al. 1993; Shimada et al. 1996; Moore and Chisholm 1999), however they usually focused on picoprokaryotes or only included individual representatives of picoeukaryotes to present a selected number of parameters.

Edwards et al. (2015) compiled photophysiological data for phytoplankton over a wide size range to identify the drivers, in particular cell size and taxonomy, of photophysiological traits, which are responsible for adaptation to the environment. Such an approach is crucial for the improvement of the parameterization of marine biogeochemical models based on plankton functional types. They showed that the affinity to light (α^{chl}) increases with cells size as a consequence of an increased packaging effect of pigments of larger cells, but they also found taxonomic or environmental influences. Further, they found a positive correlation between α^{chl} and the maximum growth rate (μ_{max}) at optimum light intensity, which they infer to be a taxonomic effect. However, they also identified this pattern for diatoms or dinoflagellates only.

They also showed a negative, however not significant trend of optimum light intensity at which growth is maximal with cell volume. In theory light saturation should increase with increasing size due to decreasing light harvesting efficiency and also decreasing photoinactivation effects in larger cells (Key et al. 2010). Steady state models were used in earlier studies to model the effects of light on the physiological response of individual phytoplankton groups (e.g., Cullen 1990; Falkowski and La Roche 1991). These models describe the photosynthesis rates in response to light under balanced growth conditions and time independent acclimated Chl *a* to carbon ratios. The photosynthesis rates are represented by an exponential function of irradiance.

A more advanced approach led to the development of dynamic photosynthesis models (e.g., Geider et al. 1997). In dynamic photosynthesis models, descriptions of both cellular carbon and Chl *a* synthesis are included. Also, the environmental feedback of the Chl *a* to carbon ratio on the photosynthesis rates is considered over time under unbalanced growth conditions (Geider et al. 1997). Chl *a* only accounts for 0.1–5% of organic biomass within phytoplankton cells (Geider et al. 1997). Despite this variability, it is still commonly used in research as an indicator for biomass because of the ease with which Chl *a* concentration can be measured by satellite or shipboard observations. Thus, the ability to describe the dynamic changes in the chlorophyll to carbon ratio of different algal groups is an important improvement, both because phytoplankton carbon cannot be measured independent of other particulate organic carbon stocks in the field, and because variability of the Chl *a* to carbon ratio is a significant contributor to (interannual) variability in ocean primary production (Buitenhuis et al. 2013).

In the present study, we will investigate the physiological response of seven strains of picophytoplankton to light, including representatives of both picoprokaryotes and picoeukaryotes. The examined picoprokaryotes will include the two main genera, Synechococcus and Prochlorococcus, including different ecotypes, while the picoeukaryotes will cover the size spectrum from 1.2 μm to 2 μm and belong to four different phytoplankton classes. To quantify the effects of light on their physiology, we will (1) quantify exponential growth rates in response to light under acclimated conditions, (2) measure the photosynthesis rates of acclimated cultures over a range of light intensities, (3) measure the Chl *a* to carbon rations of the acclimated cultures, and (4) add a dynamic representation of photoinhibition to the dynamic photosynthesis model, developed by Geider et al. (1997) to validate it with the three measured datasets for growth rates, photosynthesis rates, and Chl *a* to carbon ratios. The results will also address the question whether picoprokaryotes differ significantly from picoeukaryotes in terms of their physiological parameterization in response to light, which is relevant for their representation in marine biogeochemical models. We will further test, whether size related trends can be identified for picophytoplankton, which deviate from the current knowledge on phytoplankton photophysiology.

Material and methods

Experimental procedures and analyses

To investigate the effect of light on the exponential growth rates, photosynthesis rates and Chl *a* to carbon ratios of picophytoplankton, seven strains from diverse phytoplankton classes were obtained from the Roscoff culture collection (RCC, Vaulot et al. 2004). They include three strains belonging to the group of picoprokaryotes: *Synechococcus* sp. (RCC 30), high light (HL, RCC 296) and low light (LL, RCC162) adapted strains of *Prochlorococcus* sp., as well as four strains belonging to the group of picoeukaryotes: *Triparma eleuthera* (RCC 212), formerly known as *Bolidomonas pacifica* (Ichinomiya et al. 2016), *Micromonas pusilla* (RCC 1677), *Picochlorum* sp. (RCC 289) and *Nannochloropsis granulata* (RCC 438) (Table 1). The cell size was provided by the culture collection for six strains, and obtained from the literature for *T. eleuthera* (Guillou et al. 1999).

Of each strain, 5–7 cultures were grown in conical flasks (400 mL) in artificial seawater medium (ESAW) (Berges et al. 2001), with ammonium (882 μM $(NH_4)_2SO_4$) as the nitrogen

Table 1. Picophytoplankton strains examined in this study, including three strains of picoprokaryotes and four strains of picoeukaryotes, their Roscoff culture collection number (RCC), cell size (diameter) and location and depth of isolation.

	Species	RCC	Size (μm)	Location of isolation	Depth of isolation (m)
Picoprokaryotes	*Prochlorococcus* sp. (HL)	296	0.6	8° 32.5′N, 136° 31.8′E	150
	Prochlorococcus sp. (LL)	162	0.6	38° 59′N, 40° 33′ W	10
	Synechococcus sp.	30	1	26° 18′ N, 63° 26′W	120
Picoeukaryotes	*T. eleuthera*	212	1.2	2° 30′N, 150° 0 W	15
	M. pusilla	1677	1.5	54° 24′N, 4° 3′E	10
	Picochlorum sp.	289	2	7° 0′S, 150° 0′W	15
	N. granulata	438	2	41° 40′N, 2° 48′E	0

source and 10 nM of selenium (Na_2SeO_3). The flasks were sealed with a cotton wool stuffed linen stopper, to allow for oxygen exchange with the atmosphere.

They were placed in a Sanyo incubator (Versatile Environmental test chamber) at a constant temperature of 22°C, and acclimated to light intensities between 13 μmol photons m^{-2} s^{-1} and 720 μmol photons m^{-2} s^{-1}. The light intensities were provided by fluorescent tubes (Mitsubishi/Osram FC40ss.W/37), dimmed by neutral density film and measured with a Radiometer (Biospherical Instruments QSL-2101). The light cycle was set to 14 h of light per day. The cultures were gradually acclimated to the experimental light intensities for at least five generations before any measurements were taken, and kept in exponential growth for the duration of the experiments. For this, inocula from the 3^{rd}–7^{th} consecutive day of exponential growth, depending on the light intensity, were used and diluted to continue in exponential growth and to reduce selective processes (Lakeman et al. 2009). As the cultures did not reach stationary phases and the exchange of oxygen and inorganic carbon with the atmosphere was allowed we could also exclude potential stress effects through inorganic chemistry.

To obtain the exponential growth rates of the acclimated cultures, two 4 mL samples were taken daily and the in vivo fluorescence was measured in a Turner Design Fluorometer (10 AU) (Stawiarski et al. 2016). After 3–5 d photosynthesis rates were measured in two oxygraph systems (Hansatech Instruments Ltd, DW1/AD electrode chamber). Each oxygraph chamber was filled with a 3 mL sample of the acclimated culture and the oxygen concentration was measured continuously at a constant temperature of 21°C. There was no significant change of Chl *a* to carbon ratios between the acclimation temperature and the temperature used in the oxygraph chamber for all species (linear regression, ANOVA ($p > 0.05$), Stawiarski et al. 2016). Hence, this difference of 1°C should not affect the photosynthesis measurements. The light intensities were increased every 10 min in nine steps between 0 μmol photons m^{-2} s^{-1} and 2000 μmol photons m^{-2} s^{-1} by changing neutral density filters in front of a 3 Watt white LED lamp (Deltech GU10-1HP3W). All photosynthesis rate measurements were conducted during the exponential growth phase of the acclimated cultures after at least 6 h of light to exclude a potential effect of the day: night cycle on the Chl *a* quota and hence on the photosynthesis rates. These measurements were repeated three times for each acclimated culture with several days in-between to obtain up to 42 photosynthesis light response curves (PI-curves) per strain (5–7 acclimation light intensities $\times$ two oxygraph chambers $\times$ three replicates). Measurements from the second 5 min were used to determine the photosynthesis rate. To correct for the oxygen consumption rate by the electrodes, 3 mL of filtrate from the culture were measured in the oxygraph chambers before the photosynthesis rate measurements were taken. The oxygen consumption rate was obtained after the signal stabilized. Both *Prochlorococcus* sp. strains were filtered through polycarbonate filters (pore size 0.2 μm, Whatman), the other cultures were filtered through GF/F grade filters (nominal pore size of 0.7 μm, Whatman). The oxygen consumption rates were not statistically different (ANOVA, $p = 0.91$) between the filtrates using the two filter types, which indicates that a potentially significant influence of bacterial respiration in the culture medium can be excluded.

To obtain Chl *a* to carbon ratios, samples of both particulate organic carbon (POC) and Chl *a* were taken simultaneously with the photosynthesis rate measurements for all acclimated cultures of each strain. POC samples were collected on precombusted 13 mm GF/F grade (Whatman) filters for five strains. For samples of the *Prochlorococcus* sp. strains a layer of three filters was used, because preliminary tests showed that no cells passed through. Chl *a* samples were collected on precombusted 25 mm GF/F grade filters (Whatman) for five strains, and on 25 mm polycarbonate filters (Whatman, cyclopore track etched membrane, pore size = 0.2 μm) for the *Prochlorococcus* sp. strains. Both filter types have been shown to lead to comparable Chl *a* results using phytoplankton samples (Hashimoto and Shiomoto 2000). Both POC and Chl *a* samples were rinsed with Milli-Q water (Paulino et al. 2013), frozen in liquid nitrogen immediately after sampling and stored at −80°C until analyses.

Table 2. Definition of photophysiological parameters estimated by the dynamic photosynthesis model and other derived photophysiological parameters.

Parameter	Definition	Unit
P^C	Carbon specific rate of photosynthesis	d^{-1}
P^C_m	Carbon specific maximum rate of photosynthesis	d^{-1}
P^{Chl}_m	Chl *a* specific maximum rate of photosynthesis	g C d^{-1} (g Chl)$^{-1}$
α^{chl}	Chl *a* specific initial slope of the photosynthesis vs. irradiance curve (light affinity)	g C m^2 (g Chl mol photons)$^{-1}$
β^{Chl}	Chl *a* specific light inhibition parameter	g C m^2 (g Chl mol photons)$^{-1}$
resp	Respiration rate	d^{-1}
θ	Chl *a*:carbon ratio	g Chl *a* g^{-1} C
θ_{max}	Maximum Chl *a*:carbon ratio	g Chl *a* g^{-1} C
I_k	Light saturation of photosynthesis without light inhibition	μmol photons m^{-2} s^{-1}
I_{Opt}	Light saturation of photosynthesis with light inhibition	μmol photons m^{-2} s^{-1}
μ_{max}	Maximum growth rate at optimum light intensity	d^{-1}

The cell numbers were measured by flow cytometry (BD Biosciences FACSCalibur). The flow rate was calibrated using the method by Marie et al. (2005).

POC samples were dried for 24 h at 40°C, placed into precombusted tin capsules and analyzed with an elemental analyser (Exeter Analytical, CE-440), which was calibrated with acetanilide (Exeter Analytical). The results were corrected for medium blanks on the corresponding number of filters. The Chl *a* samples were extracted in 10 mL of acetone (Fisher Scientific, 99.8+ %), disintegrated by shaking and vortexing, and stored for 24 h in the dark at 4°C. Afterwards, the samples were centrifuged, and the fluorescence of the supernatant was measured in a Fluorescence Spectrometer (PerkinElmer LS 45). To correct for chlorophyll degradation products three drops of 8% HCl were added into the cuvette for an additional measurement. Prior to analyses, the concentration of the calibration standard (SIGMAproduct No C5753) was obtained (Parsons et al. 1984).

Calculations

For calculating the exponential growth rates (d^{-1}) of the acclimated cultures in response to light, a linear regression was applied through at least three consecutive measurements of the log-transformed in vivo fluorescence measurements. For calculating the photosynthesis rates (d^{-1}) in response to light, the measured changes in oxygen concentration over time (μmol O_2 L^{-1} s^{-1}) were converted into units of carbon production and normalized by the measured POC quota per cell. For the conversion a photosynthetic quotient of 1.1 mol O_2 mol^{-1} CO_2 was used, which is appropriate for cultures grown on ammonium as the nitrogen source (Laws 1991). Individual photosynthesis light response curves were discarded, if the photosynthesis minus respiration rate near the acclimated light intensity deviated substantially from the measured growth rates. The photosynthesis rates for the acclimated cultures of *T. eleuthera* were too low to obtain a distinct signal because of low cell densities, hence only eight reasonable photosynthesis light response curves were obtained.

To model the response of exponential growth rates, photosynthesis rates and Chl *a* to carbon ratios to light we use the dynamic photosynthesis model of Geider et al. (1997, their Eqs. 2–4). We extended their Eq. 1 with a photoinhibition term, which we obtained by reformulating the steady state light inhibition model (Platt et al. 1980) to match the dependence on a variable Chl *a* to carbon ratio in the dynamic photosynthesis model (Eqs. 1, 2).

$$\frac{\delta C}{\delta t} = P^C_m\left(1-\exp\left(\frac{-\alpha^{chl} I\theta}{P^C_m}\right)\right)\exp\left(\frac{-\beta^{Chl} I\theta}{P^C_m}\right) - \text{resp} \times C \quad (1)$$

$$\frac{\delta Chl}{\delta t} = \left(P^C_m \times \left(1-\exp\left(\frac{-\alpha^{chl} I\theta}{P^C_m}\right)\right)\exp\left(\frac{-\beta^{Chl} I\theta}{P^C_m}\right)\right)$$
$$\left(P^C_m \times \left(1-\exp\left(\frac{-\alpha^{chl} I\theta}{P^C_m}\right)\right)\exp\left(\frac{-\beta^{Chl} I\theta}{P^C_m}\right) - \text{resp}\right) \times \frac{\theta_{max}}{\alpha^{chl} I\theta} \times C \quad (2)$$

See Table 2 for an explanation of the symbols.

Five parameters (P^C_m, α^{chl}, β^{chl}, resp, θ_{max}) were estimated using a random parameter generation combined with a golden section search to minimize the residual sum of squares (RSS) between the model and measurements (Buitenhuis and Geider 2010). The three sets of measurements were: the exponential growth rates, photosynthesis rates, and the Chl *a* to carbon ratios. The data set for the photosynthesis rate measurements was larger than for the other two measurements, and had a larger relative standard deviation (RSD), hence it dominated the RSS, while the other sets of measurements, with their smaller RSD in fact provided better constraints on the parameters. The average RSD of the replicate measurements was 70% for photosynthesis rates, 11.8% for exponential growth rates, and 15.6% for the Chl *a* to carbon ratios. In addition, the contribution of the Chl *a* to carbon ratios to the RSS between the model and the measurements

was also lower because of its smaller numerical values. Therefore, exponential growth rates were weighted 50 times more in the RSS and Chl *a* to carbon ratios 30 times more than the photosynthesis rates. With these weights the contribution of exponential growth rates to the RSS was 21% ± 12%, and of Chl *a* to carbon ratios 1% ± 1%. The confidence intervals of the parameters were estimated according to Buitenhuis et al. (2013):

$$\mathrm{RSS} = \left(1.645\left(\frac{n}{n-2}\right)\left(\frac{2(2n-2)}{n(n-4)}\right) + \frac{n}{n-2}\right)\mathrm{RSS}_{\min} \tag{3}$$

In which $\mathrm{RSS}_{\min}$ is the RSS with the optimized parameter set, and each of the five parameters was varied in both the positive and negative directions until RSS reached the value set by Eq. 3. This equation was not originally formulated for using three different kinds of measurements in a single RSS, so the confidence intervals should be viewed as a relative measure of confidence, and not an exact statistical description of 95% confidence intervals.

The light saturation of photosynthesis without light inhibition (I_k) can be calculated from Eq. 4 (Talling 1957).

$$I_k = \left(\frac{\mathrm{P_m^{Chl}}}{\alpha^{\mathrm{chl}}}\right) \tag{4}$$

The light saturation of photosynthesis with light inhibition (I_{Opt}) can be calculated from Eq. 5 (Platt et al. 1980).

$$I_{\mathrm{Opt}} = \left(\frac{\mathrm{P_m^{Chl}}}{\alpha^{\mathrm{chl}}}\right)\ln\left(\frac{\alpha^{\mathrm{chl}} + \beta^{\mathrm{Chl}}}{\beta^{\mathrm{Chl}}}\right) \tag{5}$$

If β^{chl} is very low, the light saturation of photosynthesis approaches infinity. In that case it should be calculated from Eq. 4.

The Chl *a* specific maximum rate of photosynthesis ($\mathrm{P_m^{Chl}}$) can be calculated from Eq. 6.

$$\mathrm{P_m^{Chl}} = \left(\frac{\mathrm{P_m^C}}{\theta(I_{\mathrm{Opt}})}\right) \tag{6}$$

Since Eq. 6 requires I_{Opt}, the two equations were solved by iteration. The maximum growth rate (optimum growth rate at light saturation) can be calculated using Eq. 7.

$$\mu_{\max} = \mathrm{P_m^C} \times \left(\frac{14}{24}\right) - \mathrm{resp} \tag{7}$$

To test for statistically significant differences in the photosynthesis parameters between picoprokaryotes and picoeukaryotes, the Wilcoxon-Mann–Whitney-*U*-Test was used.

Results

Exponential growth rates

The measured exponential growth rates (Fig. 1, symbols) increase with increasing acclimation light intensity until they reach their maximum growth rate at light saturation for each strain. Picoeukaryotes have significantly higher ($p \leq 0.05$, $\mathrm{df} = 1$) exponential growth rates (1.2–2 $\mathrm{d^{-1}}$) around light saturation between 120 μmol photons $\mathrm{m^{-2}\ s^{-1}}$ and 500 μmol photons $\mathrm{m^{-2}\ s^{-1}}$ than picoprokaryotes (0.3–0.6 $\mathrm{d^{-1}}$) between 64 μmol photons $\mathrm{m^{-2}\ s^{-1}}$ and 330 μmol photons $\mathrm{m^{-2}\ s^{-1}}$ (Fig. 1). We also find a decline in exponential growth rates at high light intensities due to photoinhibition in both groups. *Synechococcus* sp. and the low light *Prochlorococcus* sp. strain experience the steepest decline in exponential growth rates at high light intensities. The latter is affected by photoinhibition at the lowest light intensity (147 μmol photons $\mathrm{m^{-2}\ s^{-1}}$) as compared to the other strains examined here.

We also calculate the exponential growth rates in response to acclimation light intensity by the dynamic photosynthesis model (Fig. 1, lines). The model reproduces the observed exponential growth rates well ($p < 0.01$ for all seven species). However, it tends to have a less negative or a more positive bias at the highest light intensities compared to the optimum light intensities. This bias indicates that the photoinhibition in growth rates tends to be underestimated.

Photosynthesis rates and parameters

The photosynthesis rates of the acclimated cultures of each strain (PI-curves) increase with increasing light intensity and may be affected by photoinhibition above light saturation (data not shown) as it was also found for the growth rates (Fig. 1). They are further influenced by the acclimation state of the cell, which is reflected in the Chl *a* to carbon ratio (θ). In theory, a normalization of the photosynthesis rates to θ should result in one distinct photosynthesis light response curve for each strain (Figs. 2, 3) and illustrate the decrease in light requirement with increasing θ as predicted by Eq. 1 (cf. Buitenhuis and Geider 2010).

To test whether this assumption applies to the measurements or if there is a bias in the model representation of the experimental results, the acclimated response of the individual photosynthesis curves was investigated. For this, photosynthesis parameters were calculated for all individual photosynthesis response curves using the measured Chl *a* to carbon ratios. These parameters included the maximum carbon specific rate of photosynthesis ($\mathrm{P_m^C}$), the affinity to light (α^{chl}), the light inhibition term (β^{chl}) and the respiration rate (resp) (*see* Supporting Information Fig. A1; Table A1 and Stawiarski 2014). There were no trends which would indicate a systematic bias in how the photosynthesis model represents acclimation to light intensity. For example, β^{chl} was not lowest for cultures acclimated at high light intensities and α^{chl} was not highest for cultures acclimated at low light intensities. However, some strains showed a strong variability around the mean estimates.

Finally, the dynamic photosynthesis model was applied to calculate the strain specific sets of these photosynthesis

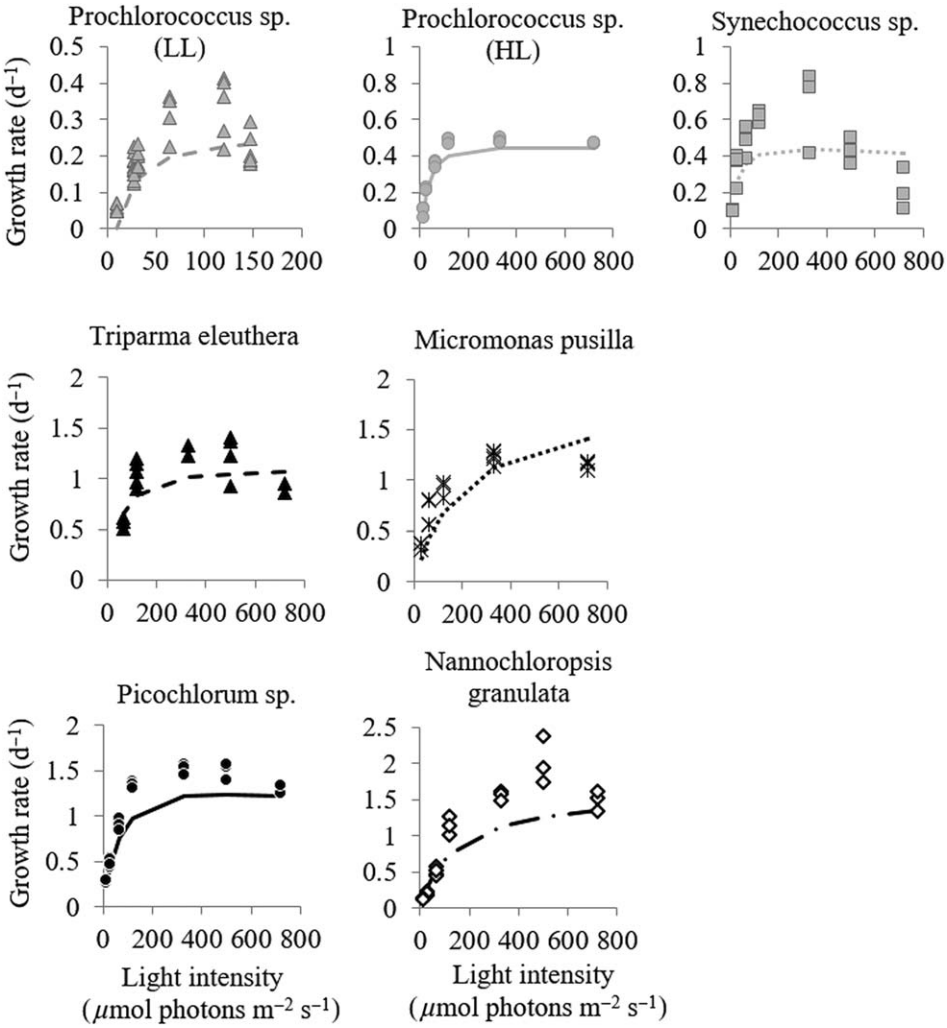

Fig. 1. Exponential growth rates of picophytoplankton as a function of light intensity. Symbols: measurements, lines: dynamic photosynthesis model fits, gray: picoprokaryotes, black: picoeukaryotes.

parameters, and also the maximum Chl *a* to carbon ratio (θ_{max}) (Table 3). It showed that for picoprokaryotes P_m^C is significantly ($p \leq 0.05$, df = 1) lower (1.00 ± 0.26 d^{-1}) than for picoeukaryotes (2.89 ± 0.63 d^{-1}) (Table 3) and increases significantly with increasing cell size ($p \leq 0.01$, $R^2 = 0.78$, Fig. 4). However, α^{chl} is higher ($p = 0.29$, df = 1) for picoprokaryotes (11.5 ± 1.4 g C m^2 (mol photons g Chl)$^{-1}$) than for picoeukaryotes (8.2 ± 6.5 g C m^2 (mol photons g Chl)$^{-1}$) (Table 3). If the outlier value of *T. eleuthera* is removed, the difference in α^{chl} between the two groups becomes significant ($p = 0.05$, df = 1) with an average α^{chl} of 5.0 ± 1.7 g C m^2 (mol photons g Chl)$^{-1}$) for the three picoeukaryotes. There is also a significant decrease of α^{chl} with cell size ($p \leq 0.05$, $R^2 = 0.73$) for the six examined strains excluding the outlier value (Fig. 4b). These trends are consistent between both, the initial acclimated approach and the dynamic photosynthesis model.

Photoinhibition is strongly present in the photosynthesis light response curves of *Synechococcus* sp. and *Picochlorum* sp. (1.46 g C m^2 (mol photons g Chl)$^{-1}$ and 0.47 g C m^2 (mol photons g Chl)$^{-1}$, respectively), while the other species have substantially lower values (Table 3). The respiration rate is higher ($p = 0.48$, df = 1) for picoprokaryotes (0.18 ± 0.16 d^{-1}) than for picoeukaryotes (0.07 ± 0.12 d^{-1}) (Table 3), again the difference is greater without *T. eleuthera* ($resp_{3picoeukaryotes} = 0.01 \pm 0.02$ d^{-1}, $p = 0.28$, df = 1). On average both of these parameter values were higher for the acclimated response. The maximum Chl *a* to carbon ratios (θ_{max}) were not significantly ($p = 0.73$, df = 1) different between the two groups (0.058 ± 0.016 g Chl (g C)$^{-1}$) (Table 3).

In addition, we calculate three photophysiological parameters from the parameters estimated by the dynamic photosynthesis model: the light saturation of photosynthesis without light inhibition (I_k, Eq. 4), the light saturation of

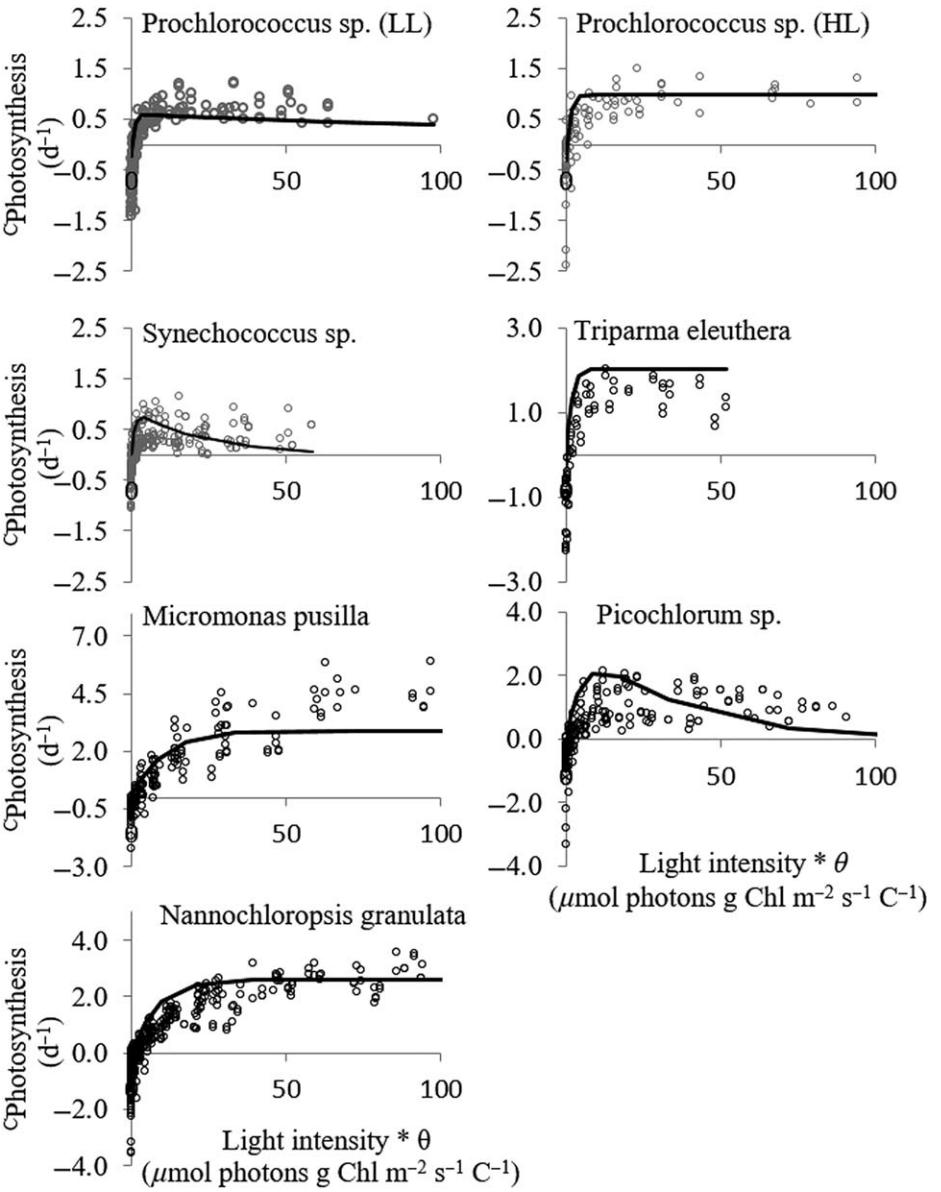

Fig. 2. Photosynthesis rates as a function of light intensity normalized to Chl *a* to carbon ratios to illustrate the decrease in light requirement with increasing θ (Eq. 1). Circles: measurements, lines: dynamic model fits, measurements and fits over the entire measured light intensity range.

photosynthesis with light inhibition (I_{Opt}, Eq. 4) and the maximum growth rate (μ_{max}, Eq. 7). Picoprokaryotes reach I_k, at significantly ($p \leq 0.05$, df =1) lower light intensities (19–45 μmol photons m^{-2} s^{-1}) than picoeukaryotes (61–274 μmol photons m^{-2} s^{-1}, Table 4). We also find a significant increase in I_k with cell size ($p \leq 0.05$, $R^2 = 0.61$, Fig. 4c). If light inhibition is included in the estimation of I_{Opt} the values are substantially higher (Table 4). Especially for strains with a very low β^{chl} the light saturation of photosynthesis is higher than the light intensities used in the experiments (> 2000 μmol photons m^{-2} s^{-1}). For μ_{max}, we find significantly ($p \leq 0.05$, df = 1) lower values for picoprokaryotes (0.41 ± 0.14 d^{-1}) than for picoeukaryotes (1.62 ± 0.46 d^{-1}) (Table 3). We also find a significant increase of μ_{max} with (1) increasing cell size for all strains ($p \leq 0.05$, $R^2 = 0.86$, Fig. 4d) and with (2) decreasing α^{chl} ($p \leq 0.05$, $R^2 = 0.72$) for six examined strains, excluding *T. eleuthera*.

We also compare the measured maximum growth rates obtained at the light intensity at which the exponential growth rates were highest to μ_{max} calculated from the photosynthesis parameters (Table 4; Fig. 4d). The measured maximum growth rates for both picoprokaryotes (0.48 ± 0.15 d^{-1}) and picoeukaryotes (1.51 ± 0.36 d^{-1}) are similar to the μ_{max} calculated from the photosynthesis parameters (Table 3; Fig.

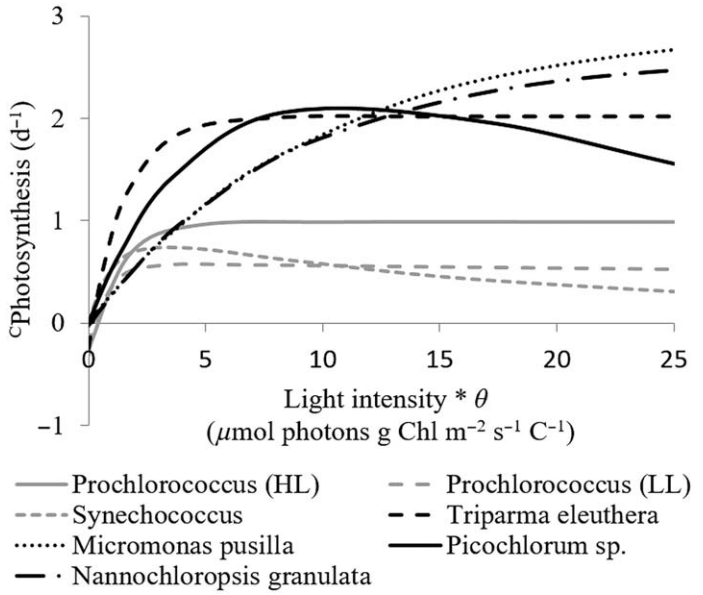

Fig. 3. Photosynthesis rates as a function of light intensity normalized to Chl *a* to carbon ratios shown at low light intensities only, lines: dynamic model fits.

4d) and also significantly ($p \leq 0.05$, df = 1) different between the groups. Further, we find an increase in maximum growth rates with cell size for the picophytoplankton strains examined here (Fig. 4d). This trend is significant for both measured μ_{max} ($p \leq 0.001$, $R^2 = 0.89$) and calculated μ_{max} ($p \leq 0.01$, $R^2 = 0.86$).

Chl *a* to carbon ratios

The Chl *a* to carbon ratios decline reciprocally with increasing light intensity in both picophytoplankton groups from 0.043 ± 0.016 g Chl g^{-1} C at 13 μmol photons m^{-2} s^{-1} to 0.014 ± 0.004 g Chl g^{-1} C at the highest acclimation light intensity of 720 μmol photons m^{-2} s^{-1} (Fig. 5). The dynamic photosynthesis model estimated θ in agreement with these measurements (Fig. 5). Only the estimates for *M. pusilla* show weaknesses in reproducing the measured maximum and minimum values. This can be explained by a low contribution of θ to the total RSS. A higher weight of θ in the parameter estimation led to a closer agreement between measurements and model and an increase in $\theta_{max}/\theta_{min}$ in this species. This higher weight was not retained because it led to less realistic results for the other photophysiological parameters of the other species.

Discussion

Exponential growth rates

The four examined picoeukaryotes have significantly higher exponential growth rates at all acclimation light intensities than the three picoprokaryotes, which is in agreement with previous studies (Malinsky-Rushansky et al. 2002;

Table 3. Photophysiological parameters and confidence intervals estimated by the dynamic photosynthesis model for the strains examined within this study.

	Size	P_m^C		α^{chl}		β^{chl}		resp		θ_{max}	
	μm	d^{-1}	±	g C m^2 (mol photons g Chl)$^{-1}$	±	g C m^2 (mol photons g Chl)$^{-1}$	±	d^{-1}	±	g Chl g^{-1} C	±
Prochlorococcus (HL)	0.6	1.3	0.01	12.14	0.61	5.48×10^{-10}	(9.87×10^{-10})*	0.31	0.01	0.086	0.004
Prochlorococcus (LL)	0.6	0.81	0.01	12.42	0.69	2.86×10^{-2}	6.67×10^{-3}	0.22	0.01	0.066	0.003
Synechococcus	1	0.9	0.01	9.81	0.38	0.47	0.02	2.64×10^{-6}	(4.74×10^{-6})*	0.041	0.002
T. eleuthera	1.2	2.27	0.03	17.71	1.00	5.27×10^{-17}	(9.49×10^{-17})*	0.25	0.01	0.044	0.002
M. pusilla	1.5	2.89	0.04	3.42	0.01	1.1×10^{-14}	(1.99×10^{-14})*	1.42×10^{-4}	(2.56×10^{-4})*	0.053	0.002
Picochlorum sp.	2	3.76	0.04	6.77	0.14	1.46	0.04	1.01×10^{-6}	(1.83×10^{-6})*	0.067	0.002
N. granulata	2	2.63	0.03	4.83	0.14	4.07×10^{-12}	(7.32×10^{-12})*	0.03	0.01	0.052	0.001

* If the lower confidence interval was < 0 only the positive confidence interval was used.

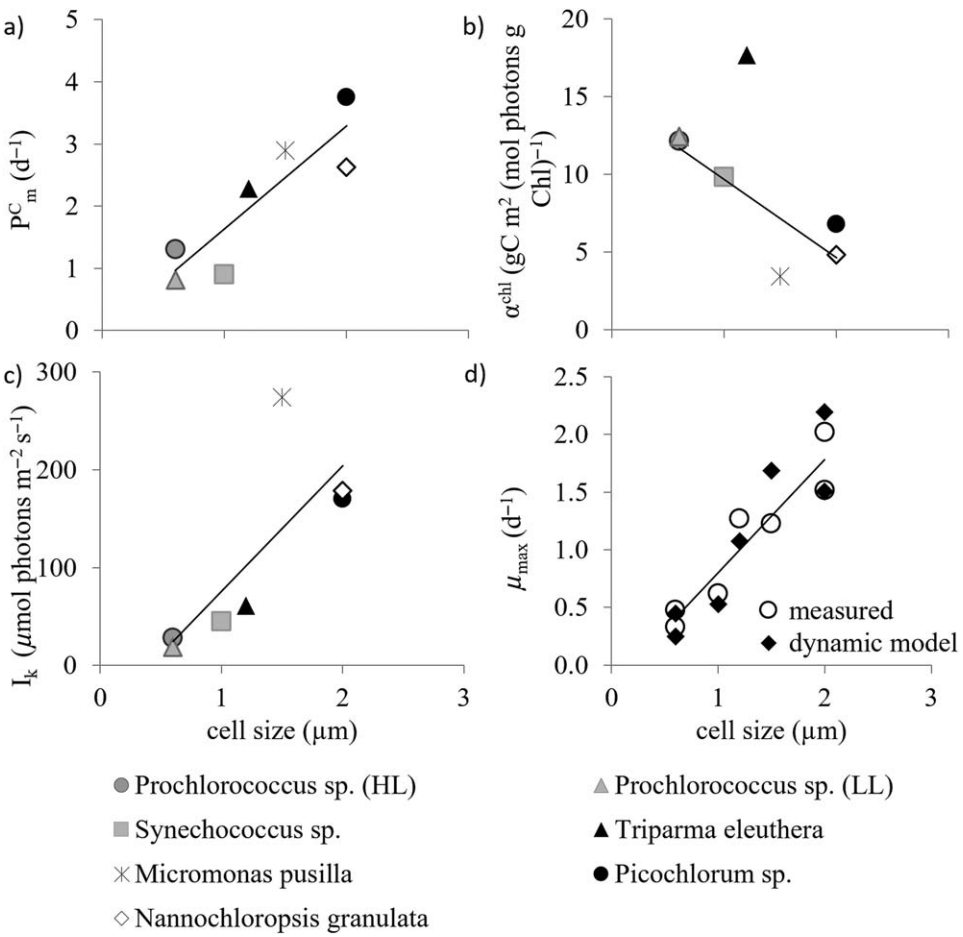

Fig. 4. Photophysiological parameters as a function of cell size: (**a**) maximum rate of photosynthesis (P^C_m), (**b**) affinity to light (α^{chl}), (**c**) light saturation of photosynthesis without photoinhibition (I_k), and (**d**) maximum growth rates (μ_{max}): circles: measured, diamonds: calculated from P^C_m and resp., lines: significant trends obtained by linear regression.

Worden et al. 2004; Morán 2007). Exponential growth rates of the low light adapted *Prochlorococcus* sp. strain are affected by photoinhibition at lower light intensities than of the high light adapted strain. This is a consequence of genetic adaptation in pigment composition to low light environments (Moore and Chisholm 1999). The *Synechococcus* sp. strain examined here also shows a steep decrease in exponential growth rates at high acclimation light intensities due to photoinhibition, which is unexpected given its general distribution shallower in the water column (Buitenhuis et al. 2012). As our strain was isolated from a depth of 120 m, we can speculate that it is a low light adapted strain.

Photophysiological parameters

The response of photosynthesis rates of picophytoplankton to light has been investigated in several studies in a variety of units (e.g., Glover et al. 1987; Partensky et al. 1993; Shimada et al. 1996; Moore and Chisholm 1999). Those studies report maximum photosynthesis rates in fg C h^{-1} (fg Chl *a*)$^{-1}$ and do not separate them from respiration rate. For a direct comparison, we converted $P^C_m - resp$ into $P^{Chl}_m - resp^{Chl}$ in the reported units (Table 4).

The results for $P^{Chl}_m - resp^{Chl}$ of the strains examined here are comparable to those of other studies for picoprokaryotes (Partensky et al. 1993; Shimada et al. 1996) and for picoeukaryotes (Glover et al. 1987; Iriarte and Purdie 1993). Also, the calculated α^{chl} is consistent with previous results (Glover et al. 1987; Partensky et al. 1993; Shimada et al. 1996; Moore and Chisholm 1999). To describe the light intensity at which photoinhibition occurs, a photoinhibition index is widely used (P^{Chl}_m/β^{chl}). Of the seven strains tested, the new dynamic photosynthesis model estimates appreciable levels of photoinhibition for two strains, which translates into a photoinhibition index of 936 μmol photons m^{-2} s^{-1} for *Synechococcus* sp. and 785 μmol photons m^{-2} s^{-1} for *Picochlorum* sp. These results are at the high end of previously reported values (Glover et al. 1987; Partensky et al. 1993). Photoinhibition was not strongly reflected in the photosynthesis measurements. The strains thus show high resistance to short-term damage through photoinhibition. In contrast to this

Table 4. Parameters calculated from the dynamic model parameters, measured and modeled maximum growth rates (μ_{max}, Eq. 7), Light saturation of photosynthesis with and without photoinhibition (I_k and I_{opt}, Eqs. 4, 5), Chl *a* to carbon ratios at optimum light intensities, and Chl *a* specific maximum rates of photosynthesis (P_m^{chl}, Eq. 6), also corrected for respiration (P_m^{chl} – $resp^{chl}$) for comparison with literature values.

	Measured		Calculated from dynamic photosynthesis model parameters					
Species	Size μm	μ_{max} d^{-1}	I_k μmol photons m^{-2} s^{-1}	I_{opt} μmol photons m^{-2} s^{-1}	θ_{Opt} g Chl (g C)$^{-1}$	μ_{max} d^{-1}	P_m^{chl} g C d^{-1} (g Chl)$^{-1}$	P_m^{chl} - $resp^{chl}$ fg C h^{-1} (fg Chl *a*)$^{-1}$.
Prochlorococcus (HL)	0.6	0.48 (±0.03)	28	660	0.045	0.45	29	1.58
Prochlorococcus (LL)	0.6	0.33 (±0.07)	19	114	0.040	0.25	20	1.04
Synechococcus	1	0.62 (±0.03)	45	140	0.024	0.53	38	2.74
T. eleuthera	1.2	1.27 (±0.07)	61	2462	0.024	1.08	93	5.93
M. pusilla	1.5	1.23 (±0.06)	274	9129	0.036	1.69	81	5.77
Picochlorum sp.	2	1.52 (±0.05)	170	293	0.038	2.19	99	7.09
N. granulata	2	2.02 (±0.14)	179	4963	0.035	1.51	74	5.26

short-term photoinhibition of the photosynthesis measurements on a time scale of minutes, long-term photoinhibition on a time scale of days led to a decrease in growth rates for six of the seven examined strains.

Light saturation of photosynthesis without light inhibition (I_k) is comparable to the previously reported range, which was lower for picoprokaryotes (Glover et al. 1987; Partensky et al. 1993; Shimada et al. 1996; Moore and Chisholm 1999) than for picoeukaryotes (Glover et al. 1987). Light saturation of photosynthesis with light inhibition (I_{Opt}) for two out of three strains of picoprokaryotes is in agreement with previous results (Partensky et al. 1993; Shimada et al. 1996). The high light adapted *Prochlorococcus* sp. strain was less affected by photoinhibition and exceeded this estimate. Only the value for *Picochlorum* sp. in the group of picoeukaryotes can be regarded as reasonable because its β^{chl} is higher than of the other strains. The I_{Opt} of the other picoeukaryote strains exceeds the light intensities used within these experiments substantially. The low representation of photoinhibition in photosynthesis measurements and consequently in the model fits suggests that I_k is a better measure than I_{Opt} for estimating the light intensity for light saturation in the investigated strains.

The maximum growth rates calculated from photophysiological parameters for two out of three picoprokaryotes are similar to those measured in other studies (Moore and Chisholm 1999; Kuan et al. 2015). We calculated a slightly lower μ_{max} for the low light adapted *Prochlorococcus* sp. strain which may be explained by strain related differences, as the temperature was chosen to be at its optimum (Stawiarski et al. 2016). The higher maximum growth rates of picoeukaryotes are consistent with previous findings (Glover et al. 1987; Six et al. 2008).

Effect of cell size on photophysiology

We find evidence for significant differences in the photophysiological parameters between both picophytoplankton groups. Picoprokaryotes have significantly lower maximum rates of photosynthesis and maximum growth rates, but significantly higher affinities for light and consequently a lower light saturation of photosynthesis. The significant continuous trends with cell size that we find here (Fig. 4) suggest that these differences may be caused by cell size rather than by taxonomic differences between prokaryotes and eukaryotes.

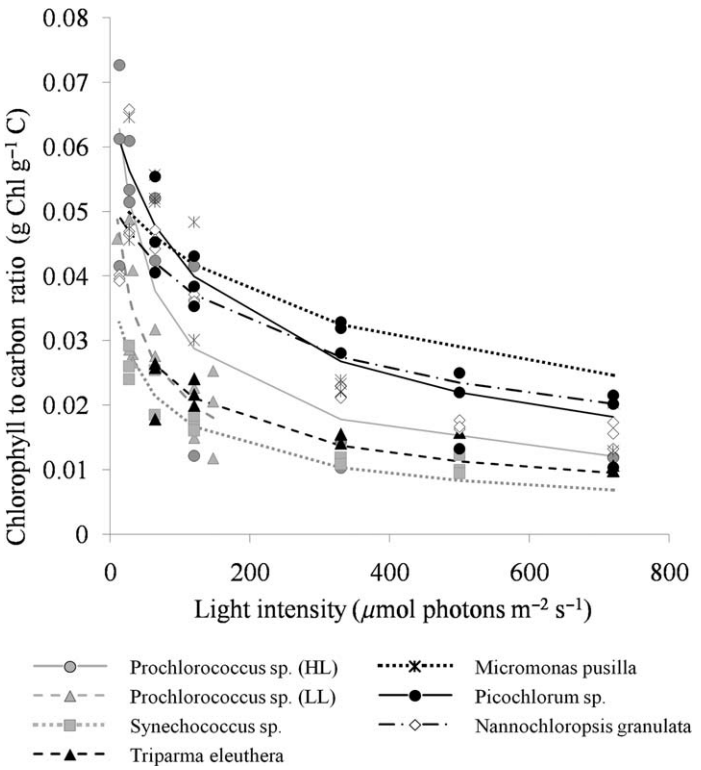

Fig. 5. Chl *a* to carbon ratios (g g^{-1}) as a function of acclimation light intensity. Symbols: measurements, lines: dynamic photosynthesis model fits.

The increasing trend for P_m^C and μ_{max} with picophytoplankton cell size has previously been described (Bec et al. 2008; Marañón et al. 2013). The increase in these rates in this phytoplankton size class can be related to the decreasing proportion of non-scalable cell components with increasing cell size (Raven 1998). It deviates from the general size-scaling rule for phytoplankton which shows a decreasing trend in maximum growth rates for cells bigger than 2–3 μm (Bec et al. 2008; Marañón et al. 2013).

In contrast, we show that α^{chl} decreases with increasing cell size. This finding is also consistent with previous findings (Edwards et al. 2015), and in agreement with theoretical assumptions related to the size of picophytoplankton. The small package effect in small cells leads to an increased efficiency in light acquisition at the expense of their maximum growth rate (Geider et al. 1986; Raven 1998). However, Edwards et al. (2015) report a positive correlation of α^{chl} with μ_{max} for phytoplankton. We show that this trend does not apply to picophytoplankton, but leads to a deviation from the general size-scaling rule for this photophysiological parameter.

Both of the above described relationships of the maximum rate of photosynthesis and of α^{chl} with cell size result in an increasing trend of light saturation of photosynthesis with cell size. This is also contrary to the results of Edwards et al. (2015), who found a negative, although not significant trend of light saturation with cell volume. In accordance with our results, it is believed that light saturation increases with increasing size due to decreasing light harvesting efficiency and also decreasing photoinactivation effects in larger cells (Key et al. 2010).

The generally higher exponential growth rates (Fig. 1) and photosynthesis rates (Figs. 2, 3) of picoeukaryotes over a wider range of light intensities may explain their high global contribution to picophytoplankton biomass of 49–68% (Buitenhuis et al. 2012). However, the higher affinity to light, lower nutrient requirements and lower grazing pressure are beneficial for picoprokaryotes in the deep chlorophyll maximum and in oligotrophic ocean regions (Chen and Liu 2010).

Field measurements show that there may be an opposite size related trend in maximum growth rates for picophytoplankton in oligotrophic ocean regions with picoprokaryotes having higher growth rates than picoeukaryotes (Taniguchi et al. 2014; Zubkov 2014). We show that even though the affinity to light is higher for picoprokaryotes, growth rates (Fig. 1) and photosynthesis rates (Figs. 2, 3) are still higher for picoeukaryotes under low light conditions. The higher in situ growth rates of picoprokaryotes in oligotrophic ocean areas may be a consequence of the better adaptation of small cells to low nutrient availability (Taniguchi et al. 2014). This is supported by the success of picoprokaryotes in competition for e.g., phosphorus (Zubkov et al. 2007) or organic nitrogen components (Zubkov et al. 2003) in oligotrophic ocean waters. Also, iron enrichment experiments have revealed that phytoplankton communities only grow at half of their maximum growth rates due to nutrient limitation (Landry et al. 2000; Laws 2013). Picoprokaryotes have been shown to dominate the picophytoplankton biomass in oligotrophic environments (Moore et al. 1995; Partensky et al. 1999*b*), but the proportion of picoeukaryotes and also the community growth rate increases with nutrient availability over a spatial and seasonal gradient (Morán 2007; Vázquez-Domínguez et al. 2013). With the dominance of picoeukaryotes, community growth rates are significantly higher (Morán 2007; Vázquez-Domínguez et al. 2013). The maximum growth rates presented here are consistent with in situ growth rates of the dominant picophytoplankton group in coastal areas (Vázquez-Domínguez et al. 2013).

The dynamic photosynthesis model

The bias in the estimation of exponential growth rates in response to light intensity by the dynamic photosynthesis model indicates that photoinhibition in exponential growth rates tends to be underestimated. This may be a consequence of the low representation of photoinhibition in the photosynthesis light response curves, which is reflected in the relatively low values of β^{chl} for five of the seven species (Table 3). Exponential growth rates may be affected by irreversible long-term damage to photosynthetic machinery during acclimation to high light intensities (on the time-scale of days), while photosynthesis rates may be affected by reversible short-term damage (on the time-scale of minutes). The dynamic photosynthesis model only represents reversible damage as a function of θ.

Also, Talmy et al. (2013) discussed potential differences in the photoacclimation potential of different phytoplankton groups due to genetic adaptation to either static or dynamic light environments. This adaptation influences their potential for allocating nitrogen to cell components associated with carbon fixation, light harvesting, photoprotection, or biosynthesis. The investment in photoprotective machinery stays higher for cells growing in dynamic light environments, even if acclimated to lower light conditions. In turn, cells, which are adapted to more stable light environments, such as *Prochlorococcus* sp. optimize their growth rates by reaching higher θ, but being more affected by photoinhibition at high light. In addition, cells which are adapted to very stable light environments, such as the *Prochlorococcus* sp. low-light ecotypes have less flexible θ (Talmy et al. 2013), which is in agreement with measurements of θ for the two *Prochlorococcus* sp. ecotypes within the present study.

Generally, picophytoplankton dominate relatively stable environments like the oligotrophic subtropical gyres. Hence, these genetic adaptations could lead to a relatively important effect of photoinhibition on photosynthesis and exponential growth rates. Thus we would suggest to explicitly distinguish between short-term and long-term damage

through photoinhibition in phytoplankton cells within dynamic photosynthesis models.

Another possible explanation for the bias in the estimation of exponential growth rates by the dynamic photosynthesis model may be missing flexibility of the respiration rate of the model. It calculates a constant respiration rate from measurements of the photosynthesis rate in the dark and applies it to the photosynthesis and exponential growth rate calculations. Since individual respiration rates were measured for each acclimated culture in the dark, it was accounted for the differences between the different acclimations with their individual growth rates. However, respiration rate may also vary with light intensity for the photosynthesis measurements. As the greater part of the residuals between the model and the data sets was explained by the photosynthesis measurements, this could be a limitation. Also, calculations of the respiration rates for individual photosynthesis curves using an acclimated approach led to much higher values with substantially higher errors than the estimate by the dynamic photosynthesis model. We would therefore suggest that the high variability in dark respiration rate measurements may have led to the uncertainty in estimating this parameter.

We show that the parameterization obtained by the dynamic photosynthesis model is able to reproduce P_m^C and α^{chl} in a range of values that have previously been reported in other studies. Hence, also the presented estimates of μ_{max} and I_k can be regarded as adequate. The estimation of μ_{max} from the dynamic model parameters was accurate and showed the same significant trend with cell size as was found in the measured maximum growth rates. We also show that it is worth to consider the contributions of both picoprokaryotes and picoeukaryotes when modeling picophytoplankton, as some of their photophysiological characteristics differ significantly. Most studies which were conducted on picophytoplankton were biased toward picoprokaryotes. Based on our results we suggest that a model parameterization with physiological parameters representative for picoprokaryotes is not appropriate for a picophytoplankton community and indicates that there is a special need to study this diverse group more thoroughly.

References

Azam, F., T. Fenchel, J. G. Field, J. S. Gray, L. A. Meyer-Reil, and F. Thingstad. 1983. The ecological role of water-column microbes in the sea. Mar. Ecol. Prog. Ser. **10**: 257–263. doi:10.3354/meps010257

Bec, B., Y. Collos, A. Vaquer, D. Mouillot, and P. Souchu. 2008. Growth rate peaks at intermediate cell size in marine photosynthetic picoeukaryotes. Limnol. Oceanogr. **53**: 863–867. doi:10.4319/lo.2008.53.2.0863

Berges, J. A., D. Franklin, and P. J. Harrison. 2001. Evolution of an artificial seawater medium: Improvements in enriched seawater, artificial water over the last two decades. J. Phycol. **37**: 1138–1145. doi:10.1046/j.1529-8817.2001.01052.x

Boyd, P. W., R. Strzepek, F. Fu, and D. A. Hutchins. 2010. Environmental control of open-ocean phytoplankton groups: Now and in the future. Limnol. Oceanogr. **55**: 1353–1376. doi:10.4319/lo.2010.55.3.1353

Buitenhuis, E. T., and R. J. Geider. 2010. A model of phytoplankton acclimation to iron – light colimitation. Limnol. Oceanogr. **55**: 714–724. doi:10.4319/lo.2010.55.2.0714

Buitenhuis, E. T., and others. 2012. Picophytoplankton biomass distribution in the global ocean. Earth Syst. Sci. Data **4**: 37–46. doi:10.5194/essd-4-37-2012

Buitenhuis, E. T., T. Hashioka, and C. Le Quéré. 2013. Combined constraints on global ocean primary production using observations and models. Global Biogeochem. Cycles **27**: 847–858. doi:10.1002/gbc.20074

Buitenhuis, E. T., and others. 2013. MAREDAT: Towards a world atlas of MARine ecosystem DATa. Earth Syst. Sci. Data **5**: 227–239. doi:10.5194/essd-5-227-2013

Chen, B., and H. Liu. 2010. Relationships between phytoplankton growth and cell size in surface oceans: Interactive effects of temperature, nutrients, and grazing. Limnol. Oceanogr. **55**: 965–972. doi:10.4319/lo.2010.55.3.0965

Cullen, J. J. 1990. On models of growth and photosynthesis in phytoplankton. Deep-Sea Res. **37**: 667–683. doi:10.1016/0198-0149(90)90097-F

Edwards, K. F., M. K. Thomas, C. A. Klausmeier, and E. Litchman. 2015. Light and growth in marine phytoplankton: Allometric, taxonomic, and environmental variation. Limnol. Oceanogr. **60**: 540–552. doi:10.1002/lno.10033

Falkowski, P. G., and J. La Roche. 1991. Acclimation to spectral irradiance in algae. J. Phycol. **27**: 8–14. doi:10.1111/j.0022-3646.1991.00008.x

Fenchel, T. 2008. The microbial loop – 25 years later. J. Exp. Mar. Biol. Ecol. **366**: 99–103. doi:10.1016/j.jembe.2008.07.013

Geider, R. J. 1987. Light and temperature dependence of the carbon to chlorophyll a ratio in microalgae and cyanobacteria: Implications for physiology and growth of phytoplankton. New Phytol. **106**: 1–34. doi:10.1111/j.1469-8137.1987.tb04788.x

Geider, R. J., T. Platt, and J. A. Raven. 1986. Size dependence of growth and photosynthesis in diatoms: A synthesis. Mar. Ecol. Prog. Ser. **30**: 93–104. doi:10.3354/meps030093

Geider, R. J., H. L. MacIntyre, and T. M. Kana. 1997. Dynamic model of phytoplankton growth and acclimation: Responses of the balanced growth rate and the chlorophyll a:carbon ratio to light, nutrient-limitation and temperature. Mar. Ecol. Prog. Ser. **148**: 187–200. doi:10.3354/meps148187

Geider, R. J., H. L. MacIntyre, and T. M. Kana. 1998. A dynamic regulatory model of phytoplanktonic acclimation to light, nutrients, and temperature. Limnol. Oceanogr. **43**: 679–694. doi:10.4319/lo.1998.43.4.0679

Glover, H. E., M. D. Keller, and R. W. Spinrad. 1987. The effects of light quality and intensity on photosynthesis and growth of marine eukaryotic and prokaryotic phytoplankton clones. J. Exp. Mar. Biol. Ecol. **105**: 137–159. doi:10.1016/0022-0981(87)90168-7

Grossman, A. R., K. R. M. Mackey, and S. Bailey. 2010. A perspective on photosynthesis in the oligotrophic oceans: Hypotheses concerning alternate routes of electron flow1. J. Phycol. **46**: 629–634. doi:10.1111/j.1529-8817.2010.00852.x

Guillou, L., M.-J. Chrétiennot-Dinet, L. K. Medlin, H. Claustre, S. Loiseaux-de Goer, and D. Vaulot. 1999. Bolidomonas: A new genus with two scpecies belonging to a new algal class, the Bolidophyceae (Heterokonta). J. Phycol. **35**: 368–381. doi:10.1046/j.1529-8817.1999.3520368.x

Hashimoto, S., and A. Shiomoto. 2000. Comparison of GF/F filters and 0.2 and 0.6 μm nuclepore filters on the chlorophyll a retention. Bull. Nat. Res. Inst. Far Seas Fish. **37**: 45–48. doi:10.1016/j.jembe.2007.01.008

Ichinomiya, M., A. L. dos Santos, P. Gourvil, S. Yoshikawa, M. Kamiya, K. Ohki, S. Audic, C. De Vargas, M.-H. Noël, D. Vaulot, and A. Kuwata. 2016. Diversity and oceanic distribution of the Parmales (Bolidophyceae), a picoplanktonic group closely related to diatoms. ISME Journal **10**: 2419–2434. doi:10.1038/ismej.2016.38

Iriarte, A., and D. A. Purdie. 1993. Photosynthesis and growth response of the oceanic picoplankter Pycnococcus provasolii Guillard (clone Ω48-23) (Chlorophyta) to variations in irradiance, photoperiod and temperature. J. Exp. Mar. Biol. Ecol. **168**: 239–251. doi:10.1016/0022-0981(93)90263-N

Key, T., A. McCarthy, D. A. Campbell, C. Six, S. Roy, and Z. V. Finkel. 2010. Cell size trade-offs govern light exploitation strategies in marine phytoplankton. Environ. Microbiol. **12**: 95–104. doi:10.1111/j.1462-2920.2009.02046.x

Kuan, D., S. Duff, D. Posarac, and X. Bi. 2015. Growth optimization of Synechococcus elongatus PCC7942 in lab flasks and a 2-D photobioreactor. Can. J. Chem. Eng. **93**: 640–647. doi:10.1002/cjce.22154

Lakeman, M. B., P. von Dassow, and R. A. Cattolico. 2009. The strain concept in phytoplankton ecology. Harmful Algae **8**: 746–758. doi:10.1016/j.hal.2008.11.011

Landry, M. R., M. E. Ondrusek, S. J. Tanner, S. L. Brown, J. Constantinou, R. R. Bidigare, K. H. Coale, and S. Fitzwater. 2000. Biological response to iron fertilization in the eastern equatorial Pacific (IronEx II). I. Microplankton community abundances and biomass. Mar. Ecol. Prog. Ser. **201**: 27–42. doi:10.3354/meps201027

Laws, E. A. 1991. Photosynthetic quotients, new production and net community production in the open ocean. Deep-Sea Res. **38**: 143–167. doi:10.1016/0198-0149(91)90059-O

Laws, E. A. 2013. Evaluation of in situ phytoplankton growth rates: A synthesis of data from varied approaches. Ann. Rev. Mar. Sci. **5**: 247–268. doi:10.1146/annurev-marine-121211-172258

Malinsky-Rushansky, N., T. Berman, T. Berner, Y. Z. Yacobi, and Z. Dubinsky. 2002. Physiological characteristics of picophytoplankton, isolated from Lake Kinneret: Responses to light and temperature. J. Plankton Res. **24**: 1173–1183. doi:10.1093/plankt/24.11.1173

Marañón, E., P. Cermeño, D. C. López-Sandoval, T. Rodríguez-Ramos, C. Sobrino, M. Huete-Ortega, J. M. Blanco, and J. Rodríguez. 2013. Unimodal size scaling of phytoplankton growth and the size dependence of nutrient uptake and use. Ecol. Lett. **16**: 371–379. doi:10.1111/ele.12052

Marie, D., N. Simon, and D. Vaulot. 2005. Phytoplankton cell counting by flow cytometry, p. 253–267. *In* R. Andersen [ed.], Algal culturing techniques. Elsevier/Academic Press.

Massana, R., and R. Logares. 2013. Eukaryotic versus prokaryotic marine picoplankton ecology. Environ. Microbiol. **15**: 1254–1261. doi:10.1111/1462-2920.12043

Moore, L. R., R. Goericke, and S. W. Chisholm. 1995. Comparative physiology of Synechococcus and Prochlorococcus: Influence of light and temperature on growth, pigments, fluorescence and absorptive properties. Mar. Ecol. Prog. Ser. **116**: 259–275. doi:10.3354/meps116259

Moore, L. R., and S. W. Chisholm. 1999. Photophysiology of the marine cyanobacterium Prochlorococcus: Ecotypic differences among cultured isolate. Limnol. Oceanogr. **44**: 628–638. doi:10.3354/meps116259

Morán, X. A. G. 2007. Annual cycle of picophytoplankton photosynthesis and growth rates in a temperate coastal ecosystem: A major contribution to carbon fluxes. Aquat. Microb. Ecol. **49**: 267–279. doi:10.3354/ame01151

Morán, X. A. G., Á. López-Urrutia, A. Calvo-Díaz, and W. K. W. Li. 2010. Increasing importance of small phytoplankton in a warmer ocean. Glob. Chang. Biol. **16**: 1137–1144. doi:10.1111/j.1365-2486.2009.01960.x

Parsons, T. R., Y. Maita, and C. M. Lalli. 1984. A Manual of Chemical and Biological Methods for Seawater Analysis. Pergamon Press, Oxford, 173 pp.

Partensky, F., N. Hoepffner, W. K. W. Li, O. Ulloa, and D. Vaulot. 1993. Photoacclimation of Prochlorococcus sp. (Prochlorophyta) strains isolated from the North Atlantic and the Mediterranean Sea. Plant Physiol. **101**: 285–296. doi:10.1104/pp.101.1.285

Partensky, F., D. Blanchot, and D. Vaulot. 1999. Differential distribution and ecology of Prochlorococcus and Synechococcus in oceanic waters: a review. Bull. Inst. Oceanogr. Monaco Numero Spec. **19**: 457–475.

Paulino, A. I., M. Heldal, S. Norland, and J. K. Egge. 2013. Elemental stoichiometry of marine particulate matter measured by wavelength dispersive X-ray fluorescence (WDXRF) spectroscopy. J. Mar. Biol. Assoc. U.K. **93**: 2003–2014. doi:10.1017/S0025315413000635

Platt, T., C. L. Gallegos, and W. Glen Harrison. 1980. Photoinhibition and photosynthesis in natural assemblages of marine phytoplankton. J. Mar. Res. **38**: 687–701.

Raven, J. 1998. The twelfth Tansley Lecture. Small is beautiful: The picophytoplankton. Funct. Ecol. **12**: 503–513. doi:10.1046/j.1365-2435.1998.00233.x

Shimada, A., T. Maruyama, and S. Miyachi. 1996. Vertical distributions and photosynthetic action spectre of two oceanic picophytopianlcters, Prochlorococcus Marinus and Synechococcus sp. Mar. Biol. **127**: 15–23. doi:10.1007/BF00993639

Six, C., Z. V. Finkel, F. Rodriguez, D. Marie, F. Partensky, and D. A. Campbell. 2008. Contrasting photoacclimation costs in ecotypes of the marine eukaryotic picoplankter Ostreococcus. Limnol. Oceanogr. **53**: 255–265. doi:10.4319/lo.2008.53.1.0255

Stawiarski, B. 2014. The physiological response of picophytoplankton to light, temperature and nutrients, including climate change model simulations. Ph.D. thesis. Univ. of East Anglia.

Stawiarski, B., E. T. Buitenhuis, and C. Le Quéré. 2016. The physiological response of picophytoplankton to temperature and its model representation. Front. Mar. Sci. **3**: 164. doi:10.3389/fmars.2016.00164

Sterner, R. W., and J. J. Elser. 2002. Ecological stoichiometry: The biology of elements from molecules to the biosphere. Princeton Univ. Press.

Talmy, D., J. Blackford, N. J. Hardman-Mountford, A. J. Dumbrell, and R. J. Geider. 2013. An optimality model of photoadaptation in contrasting aquatic light regimes. Limnol. Oceanogr. **58**: 1802–1818. doi:10.4319/lo.2013.58.5.1802

Taniguchi, D. A. A., M. R. Landry, P. J. S. Franks, and K. E. Selph. 2014. Size-specific growth and grazing rates for picophytoplankton in coastal and oceanic regions of the eastern Pacific. Mar. Ecol. Prog. Ser. **509**: 87–101. doi:10.3354/meps10895

Vaulot, D., F. Le Gall, D. Marie, L. Guillou, and F. Partensky. 2004. The Roscoff Culture Collection (RCC): A collection dedicated to marine picoplankton. Nova Hedwigia **79**: 49–70. doi:10.1127/0029-5035/2004/0079-0049

Vaulot, D., W. Eikrem, M. Viprey, and H. Moreau. 2008. The diversity of small eukaryotic phytoplankton (< 3 μm) in marine ecosystems. FEMS Microbiol. Rev. **32**: 795–820. doi:10.1111/j.1574-6976.2008.00121.x

Vázquez-Domínguez, E., X. Morán, and A. López-Urrutia. 2013. Photoacclimation of picophytoplankton in the central Cantabrian Sea. Mar. Ecol. Prog. Ser. **493**: 43–56. doi:10.3354/meps10549

Veldhuis, M. J. W., K. R. Timmermans, P. Croot, and B. Van der Wagt. 2005. Picophytoplankton; a comparative study of their biochemical composition and photosynthetic properties. J. Sea Res. **53**: 7–24. doi:10.1016/j.seares.2004.01.006

Worden, A. Z., J. K. Nolan, and B. Palenik. 2004. Assessing the dynamics and ecology of marine picophytoplankton: The importance of the eukaryotic component. Limnol. Oceanogr. **49**: 168–179. doi:10.4319/lo.2004.49.1.0168

Zubkov, M. V. 2014. Faster growth of the major prokaryotic versus eukaryotic CO2 fixers in the oligotrophic ocean. Nat. Commun. **5**: 3776. doi:10.1038/ncomms4776

Zubkov, M. V., B. M. Fuchs, G. A. Tarran, P. H. Burkill, and R. Amann. 2003. High rate of uptake of organic nitrogen compounds by Prochlorococcus cyanobacteria as a key to their dominance in oligotrophic oceanic waters. Appl. Environ. Microbiol. **69**: 1299–1304. doi:10.1128/AEM.69.2.1299

Zubkov, M. V., I. Mary, E. M. S. Woodward, P. E. Warwick, B. M. Fuchs, D. J. Scanlan, and P. H. Burkill. 2007. Microbial control of phosphate in the nutrient-depleted North Atlantic subtropical gyre. Environ. Microbiol. **9**: 2079–2089. doi:10.1111/j.1462-2920.2007.01324.x

Acknowledgments

We would like to thank Professor Corinne Le Quéré for continuous support and critical comments. We also thank Robert Utting for technical support in the laboratory at any time. The research leading to these results has received funding from the European Community's Seventh Framework Programme (FP7 2007-2013) under grant agreement n° 238366 (Greencycles II), and the Natural Environment Research Council grant n° NE/K001302/1(i-MarNet). The data sets and the program for estimating the photosynthetic parameters are available in the supporting Information online.

Conflict of Interest

None declared.

Submitted 31 March 2017
Revised 03 September 2017
Accepted 10 October 2017

Associate editor: Heidi Sosik